



## Improved modelling of a MEMS transducer with a planar micro- beam and a reduced-size backplate

Petr Honzík, Antonin Novak, Stéphane Durand, Nicolas Joly, Michel Bruneau

### ► To cite this version:

Petr Honzík, Antonin Novak, Stéphane Durand, Nicolas Joly, Michel Bruneau. Improved modelling of a MEMS transducer with a planar micro- beam and a reduced-size backplate. Forum Acusticum, Dec 2020, Lyon, France. pp.2535-2538, 10.48465/fa.2020.0642 . hal-03231877

**HAL Id: hal-03231877**

**<https://hal.science/hal-03231877>**

Submitted on 21 May 2021

**HAL** is a multi-disciplinary open access archive for the deposit and dissemination of scientific research documents, whether they are published or not. The documents may come from teaching and research institutions in France or abroad, or from public or private research centers.

L'archive ouverte pluridisciplinaire **HAL**, est destinée au dépôt et à la diffusion de documents scientifiques de niveau recherche, publiés ou non, émanant des établissements d'enseignement et de recherche français ou étrangers, des laboratoires publics ou privés.

# IMPROVED MODELLING OF A MEMS TRANSDUCER WITH A PLANAR MICRO-BEAM AND A REDUCED-SIZE BACKPLATE

Petr Honzík<sup>1</sup>

Antonin Novák<sup>2</sup>

Stéphane Durand<sup>2</sup>

Nicolas Joly<sup>2</sup>

Michel Bruneau<sup>2</sup>

<sup>1</sup> Faculty of Transportation Sciences, Czech Technical University in Prague, Czech Republic

<sup>2</sup> Laboratoire d'Acoustique de l'Université du Mans UMR CNRS 6613, Université du Mans, France.

honzikp@fd.cvut.cz

## ABSTRACT

Based on recently published analytical models of miniaturized transducers containing planar micro-beams, this contribution deals with an improved model of such devices. Owing to the presence of the reduced-size backplate in the device considered herein, the acoustic system loading the micro-beam contains two parts of different thickness with a geometrical discontinuity between them. The analytical modelling presented herein takes into account the spatial dependence of the acoustic pressure in both of these parts, while the previous models supposed a cavity-like behaviour (uniform acoustic pressure) of the thicker part. Moreover, effects of sharp edges at the boundary between the thin slits surrounding the micro-beam and these two parts are taken into account in using an added mass approximation. A rigid micro-beam attached at one end to a flexible hinge is considered in this study. The displacement of the micro-beam along with the sensitivity of the transducer are calculated and compared with the reference numerical (FEM) solution.

## 1. INTRODUCTION

Fully analytical models of one-dimensional acoustic devices containing planar beams (rigid elastically supported or attached at one end to a flat spring, miniaturized or not) loaded with a thin fluid layer with discontinuity in thickness have been published recently [1–5]. The use of such devices as MEMS transducers with reduced-size backplate is of interest because of their geometrical simplicity, hence lower fabrication complexity and cost. The use of reduced-size backplate improves the compactness of the device (the backing reservoir is directly under the moving electrode) and enables to adjust more geometrical parameters in order to optimize the behaviour of the transducer [6]. The above mentioned models generally suffer from slightly underestimated damping because of neglected effects of sharp edges at the entering to the fluid gap through thin slits surrounding the beam and from slightly shifted resonant frequency (when under-damped), which is related to the assumption of uniform acoustic pressure in thicker parts of the fluid gap (cavity approximation). An improved analytical model of such devices is proposed herein, where the problem of sharp edges is taken into account by an approximate man-

ner using an added mass and where a one-dimensional analytical expression for the non-uniform acoustic pressure is used for all parts of the fluid gap. As for the previous models, the thermal and viscous boundary layer effects [7] are taken into account in all parts of the fluid gap and the thin slits surrounding the beam. The mean displacement of the beam over the surface of the fixed electrode and the corresponding acoustic pressure sensitivity of the transducer are calculated and compared to the reference results of full 3D numerical (FEM) simulation [8], and the discrepancies are then discussed.

## 2. ANALYTICAL APPROACH

The device (Fig. 1) contains the planar rigid micro-beam of dimensions  $L \times b \times h_b$  (length  $\times$  width  $\times$  thickness) connected to a micro-hinge at the left side and free at the right side. The micro-beam is surrounded by two thin air-filled slits of thickness  $h_s$ , one slit of thickness  $h_L$  at  $x = L$  and

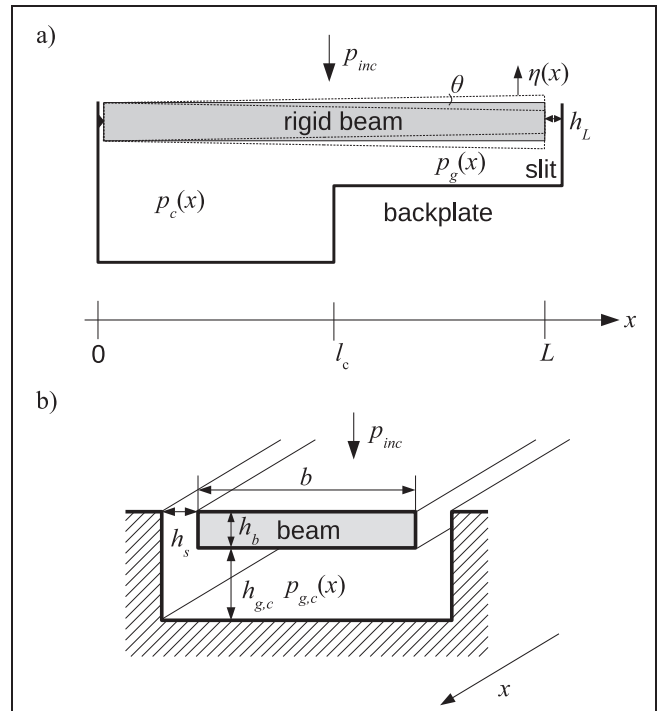


**Figure 1.** Geometry of the system: a) side view, b) cross-sectional view.

loaded by a fluid layer with discontinuity in thickness. For the part on the length interval  $x \in (0, l_c)$  this thickness is designated by  $h_c$ , while the thickness of the other part ( $x \in (l_c, L)$ ) is designated by  $h_g$ . The incident acoustic pressure  $p_{inc}$  with harmonic ( $e^{i\omega t}$ ) time dependence ( $\omega$  is the angular velocity) excites the displacement of the beam  $\eta(x) = \theta x$  ( $\theta$  being the angle of the beam), which is coupled with the acoustic pressure  $p_c(x) \forall x \in (0, l_c)$  and  $p_g(x) \forall x \in (l_c, L)$  inside the transducer.

## 2.1 Effect of sharp edges

The particle velocity entering to the air gap through the lateral slit averaged on the thickness of the slit can be expressed as [2]

$$\bar{v}_{s,y}(x) = -\frac{1}{i\omega\rho_0} \frac{p_{inc} - p_{g,c}(x)}{h_b} F_{v,s} + \frac{1}{2} i\omega\eta(x) K_{v,s}, \quad (1)$$

where  $\rho_0$  is the air density,  $F_{v,s}$  and  $K_{v,s}$  are associated with the mean profile of the particle velocity in the slit (due to the air viscosity), see [2]. In case of blocked micro-beam ( $\eta = 0$ ), Eqn. (1) can be rewritten in order to obtain the specific impedance of the slit

$$Z_s = \frac{p_{g,c}(x) - p_{inc}}{\bar{v}_{s,y}(x)} = i\omega \frac{\rho_0 h_b}{F_{v,s}}, \quad (2)$$

which is an impedance of a specific mass. The sharp edge effects can be then approximately taken into account by including a specific added mass  $M_{Sadd}$  to this mass

$$M_{slit} = \frac{\rho_0 h_b}{F_{v,s}} + M_{Sadd}. \quad (3)$$

Eqn. (1) can be then rewritten as follows:

$$\bar{v}_{s,y}(x) = -\frac{p_{inc} - p_{g,c}(x)}{i\omega M_{slit}} + \frac{1}{2} i\omega\eta(x) K_{v,s}. \quad (4)$$

A rough estimate of the added mass originating from the low frequency approximation of the radiation impedance [7]

$$M_{Sadd} = \frac{8\rho_0\sqrt{h_s L}}{3\sqrt{\pi^3}} \quad (5)$$

is used herein.

## 2.2 Equations governing the acoustic pressure inside the device

Following the same procedure as in [2] leads to wave equation governing the acoustic pressure in both parts of the air gap, the subscripts  $c$  and  $g$  designate the thicker part ( $x \in (0, l_c)$ ) and the thinner part ( $x \in (l_c, L)$ ) of the air gap respectively

$$\left( \frac{\partial^2}{\partial x^2} + \chi_{g,c}^2 \right) p_{g,c}(x) = -[U_{1(g,c)} p_{inc} + U_{2(g,c)} \eta(x)], \quad (6)$$

with the complex wavenumbers  $\chi_{g,c}$  taking into account the thermo-viscous effects in the air gap and the coefficients  $U_{1(g,c)}$  and  $U_{2(g,c)}$  in the right hand side of Eqn. (6)

taken from [2], only the term  $\frac{F_{v,s} h_s}{F_{v,g} h_g h_b b}$  is replaced by  $\frac{\rho_0 h_s}{M_{slit} F_{v,g} h_g h_b b}$  due to Eqn. (4).

The classical solution of Eqn. (6) is considered

$$p_{g,c}(x) = A_{g,c} \cos(\chi_{g,c} x) + B_{g,c} \sin(\chi_{g,c} x) - \frac{1}{\chi_{g,c}^2} [U_{1(g,c)} p_{inc} + U_{2(g,c)} \theta x], \quad (7)$$

along with four boundary conditions

$$\begin{aligned} x = 0 : \quad & \partial_x p_c(0) = 0, \\ x = l_c : \quad & p_c(l_c) = p_g(l_c), \\ & w_c(l_c) = w_g(l_c), \\ x = L : \quad & w_g(L) = \bar{v}_{L,y} h_L b, \end{aligned} \quad (8)$$

where  $w_{g,c}$  are the volume velocities in both parts of the acoustic system behind the micro-beam. The first boundary condition leads directly to the expression of the integration constant  $B_c = \frac{U_{2c}}{\chi_c^2} \theta$ , the other integration constants  $A_g$ ,  $B_g$  and  $A_c$  have to be calculated from the solution of the system of three equations given by the three remaining boundary conditions from Eqn. (8).

When the expressions for the acoustic pressure inside the device are found, it remains to follow the same procedure as in [4], e.g. to substitute this expression for the acoustic pressure into the relation for the angle  $\theta$  of the micro-beam (Eqn. (1) in [4]) which involve the mass moment of inertia  $J_b = m_b L^2/3$  ( $m_b$  being the mass of the micro-beam), the force moment  $C_b$  and the damping coefficient of the hinge  $D_b$  (neglected herein  $D_b = 0$ ). The mean displacement of the micro-beam over the surface of the backplate  $\bar{\eta} = \theta(L + l_c)/2$  can be then calculated.

## 3. RESULTS

In this section the acoustic pressure sensitivity  $\sigma = U_0 \bar{\eta} / (p_{inc} h_g)$  of the device used as electrostatic transducer with polarization voltage  $U_0$  is presented. The dimensions and other parameters of the device are summarized in Tab. 1, the properties of the air are given in Tab. 2.

Parameter	Value	Unit
Beam length $L$	$3 \times 10^{-3}$	m
Beam width $b$	$0.4 \times 10^{-3}$	m
Beam thickness $h_b$	$50 \times 10^{-6}$	m
Cavity length $l_c$	$3L/4$	m
Cavity thickness $h_c$	$150 \times 10^{-6}$	m
Airgap thickness $h_g$	$50 \times 10^{-6}$	m
Thickness of the slits $h_s$	$2 \times 10^{-6}$	m
Density (silicon) $\rho_b$	2329	kg/m <sup>3</sup>
Force moment $C_b$	$1.0916 \times 10^{-4}$	N m
Polarization voltage $U_0$	30	V

**Table 1.** Dimensions and other parameters of the device.

Fig. 2 shows the magnitude and phase of the acoustic pressure sensitivity of the transducer. The result of the model presented herein (red curve) is compared with the

Parameter	Value	Unit
Static pressure $P_0$	101330	Pa
Static temperature $T_0$	293.15	K
Density $\rho_0$	1.204	kg/m <sup>3</sup>
Adiabatic speed of sound $c_0$	343.2	m/s
Shear dynamic viscosity $\mu$	$1.814 \times 10^{-5}$	Pa s
Bulk dynamic viscosity $\mu_B$	$1.088 \times 10^{-5}$	Pa s
Thermal conductivity $\lambda_h$	$25.77 \times 10^{-3}$	W/(mK)
Ratio of specific heats $\gamma$	1.400	-
Specific heat coefficient at constant pressure per unit of mass $C_P$	1005	J/(kgK)

**Table 2.** Parameters of the thermo-viscous fluid (air).

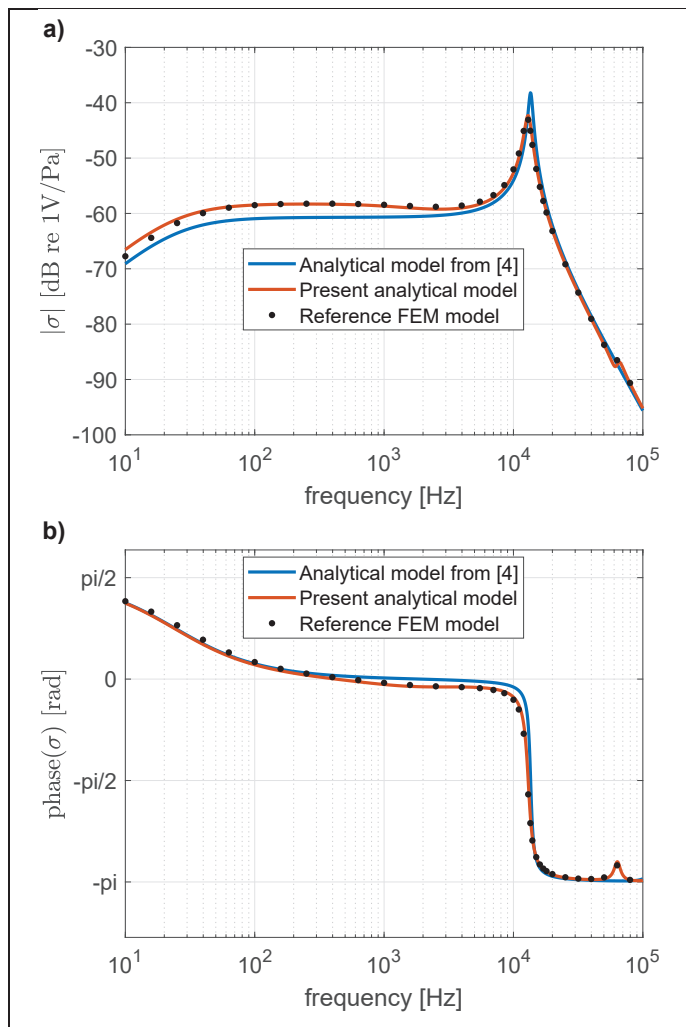


**Figure 2.** Magnitude a) and phase b) of the transducer sensitivity: comparison between previous model [4] (blue curve), present model (red curve) and the reference numerical (FEM) solution (black points).

result of previous model [4] (blue curve) and with a reference numerical result of full 3D FEM simulation (based on

method and software described in [8]) (black points). The present model is in very good agreement with the reference FEM model while the previous model shows some discrepancies from the reference both in the level of sensitivity in the flat part of the curve and in the damping at resonance frequency.

## 4. CONCLUSIONS

The behaviour of the miniaturized transducer consisting of a planar rigid micro-beam attached at one end to a flexible hinge and a reduced-size backplate has been studied and the improved analytical model of such device has been developed. Comparing to previous models, the spatial dependence of the acoustic pressure along the  $x$  axis inside the device is completely taken into account. Additionally, the effects of the sharp edges at the boundary of the thin slits surrounding the micro-beam has been also modelled by an approximate manner using an added mass. The present model shows better agreement with the reference numerical (FEM) model than the previous one. This enables the use of such a model in design of new types of miniaturized acoustic receivers (MEMS microphones).

## 5. ACKNOWLEDGEMENTS

This work was supported by the Grant Agency of the Czech Technical University in Prague, grant No. SGS18/200/OHK2/3T/16.

## 6. REFERENCES

- [1] T. Verdot, E. Redon, K. Ege, J. Czarny, C. Guianvarc'h, J.-L. Guyader, Microphone with planar nano-gauge detection: fluid-structure coupling including thermoviscous effects, *Acta Acust. U. Acust.* 102(3)(2016), 517–529.
- [2] A. Novák, P. Honzík, M. Bruneau, Dynamic behaviour of a planar micro-beam loaded by a fluid-gap: analytical and numerical approach in a high frequency range, benchmark solutions, *J. Sound Vib.* **401** (2017), 36–53.
- [3] L. Ehrig, H. Schenk, S. Langa, A. Melnikov, M. Stolz, B. Kaiser, H. Conrad, H. Schenk, Electrostatic All-Silicon MEMS Speakers for In-Ear Audio Applications - Acoustic Measurements and Modelling Approach, *Proc. of ICA 2019*, p. 7339–7344, Aachen, Germany, September 2019.
- [4] P. Honzík, A. Novák, S. Durand, N. Joly, M. Bruneau, Analytical modelling of a MEMS transducer composed of a rigid micro-beam attached at one end to a flat spring moving against a reduced-size backplate, *Proc. of ICA 2019*, p. 7375–7381, Aachen, Germany, September 2019.
- [5] P. Honzík, A. Novák, S. Durand, N. Joly, M. Bruneau, Modeling of a one-dimensional acoustic device composed of a planar beam and fluid gap with discontinuity

in thickness, Proc. of Meetings on Acoustics **30** (2017), 030016.

- [6] P. Honzík, A. Podkovskiy, S. Durand, N. Joly, M. Bruneau, Analytical and numerical modeling of an axisymmetrical electrostatic transducer with interior geometrical discontinuity, J. Acoust. Soc. Am. **134** (2013), 3573-3579.
- [7] M. Bruneau, T. Scelo (translator and contributor), *Fundamentals of Acoustics* (ISTE, London, 2006).
- [8] M. J. Herring Jensen, E. Sandermann Olsen, Virtual prototyping of condenser microphone using the finite element method for detailed electric, mechanic, and acoustic characterisation, Proc. of Meetings on Acoustics **19** (2013), 030039.